cells

MDPI

Article

Two-Step In Vitro Model to Evaluate the Cellular Immune Response to SARS-CoV-2

Juliana G. Melgaço [1,*,†,‡], Tamiris Azamor [1,†], Andréa M. V. Silva [1], José Henrique R. Linhares [1], Tiago P. dos Santos [1], Ygara S. Mendes [1], Sheila M. B. de Lima [1], Camilla Bayma Fernandes [1], Jane da Silva [1], Alessandro F. de Souza [1], Luciana N. Tubarão [1], Danielle Brito e Cunha [1], Tamires B. S. Pereira [1], Catarina E. L. Menezes [1], Milene D. Miranda [2], Aline R. Matos [2], Braulia C. Caetano [2], Jéssica S. C. C. Martins [2], Thyago L. Calvo [3], Natalia F. Rodrigues [4,5], Carolina Q. Sacramento [4,5], Marilda M. Siqueira [2], Milton O. Moraes [3], Sotiris Missailidis [1], Patrícia C. C. Neves [1] and Ana Paula D. Ano Bom [1]

[1] Instituto de Tecnologia em Imunobiológicos, Bio-Manguinhos, Fundação Oswaldo Cruz, FIOCRUZ, Rio de Janeiro 21040-900, Brazil; tamiris.azamor@bio.fiocruz.br (T.A.); amarques@bio.fiocruz.br (A.M.V.S.); jose.henrique@bio.fiocruz.br (J.H.R.L.); tiago.pereira@bio.fiocruz.br (T.P.d.S.); ygara.mendes@bio.fiocruz.br (Y.S.M.); smaria@bio.fiocruz.br (S.M.B.d.L.); camilla.bayma@bio.fiocruz.br (C.B.F.); jane.silva@bio.fiocruz.br (J.d.S.); fonseca@bio.fiocruz.br (A.F.d.S.); luciana.tubarao@bio.fiocruz.br (L.N.T.); danielle.cunha@bio.fiocruz.br (D.B.e.C.); tbomfimsantos@gmail.com (T.B.S.P.); menezescat@outlook.com (C.E.L.M.); sotiris.missailidis@bio.fiocruz.br (S.M.); Pcristina@bio.fiocruz.br (P.C.C.N.); adinis@bio.fiocruz.br (A.P.D.A.B.)

[2] Laboratório de Vírus Respiratório e do Sarampo, Instituto Oswaldo Cruz, Fundação Oswaldo Cruz, FIOCRUZ, Rio de Janeiro 21040-900, Brazil; milene_dias@yahoo.com.br (M.D.M.); alinematos@hotmail.com (A.R.M.); braulia.costa@gmail.com (B.C.C.); jessicadl_10@hotmail.com (J.S.C.C.M.); mmsiq@ioc.fiocruz.br (M.M.S.)

[3] Laboratório de Hanseníase, Instituto Oswaldo Cruz, Fundação Oswaldo Cruz, FIOCRUZ, Rio de Janeiro 21040-900, Brazil; thyagoleal@yahoo.com (T.L.C.); milton.moraes@fiocruz.br (M.O.M.)

[4] Laboratório de Imunofarmacologia, Instituto Oswaldo Cruz, Fundação Oswaldo Cruz, FIOCRUZ, Rio de Janeiro 21040-900, Brazil; nataliafintelman@gmail.com (N.F.R.); carol.qsacramento@gmail.com (C.Q.S.)

[5] Centro de Desenvolvimento Tecnológico em Saúde, Fundação Oswaldo Cruz, FIOCRUZ, Rio de Janeiro 21040-900, Brazil

* Correspondence: juliana.melgaco@bio.fiocruz.br; Tel.: +55-21-3882-9493

† Authors contributed equally.

‡ Current address: Room 414, 4th Floor, Rocha Lima Building, Avenida Brasil, 4365, Manguinhos, Rio de Janeiro 21040-900, Brazil.

check for updates

Citation: Melgaço, J.G.; Azamor, T.; Silva, A.M.V.; Linhares, J.H.R.; dos Santos, T.P.; Mendes, Y.S.; de Lima, S.M.B.; Fernandes, C.B.; da Silva, J.; de Souza, A.F.; et al. Two-Step In Vitro Model to Evaluate the Cellular Immune Response to SARS-CoV-2. *Cells* **2021**, *10*, 0. https://doi.org/

Academic Editor: Isabella Quinti

Received: 29 July 2021
Accepted: 6 August 2021
Published: 11 August 2021

Publisher's Note: MDPI stays neutral with regard to jurisdictional claims in published maps and institutional affiliations.

Abstract: The cellular immune response plays an important role in COVID-19, caused by SARS-CoV-2. This feature makes use of in vitro models' useful tools to evaluate vaccines and biopharmaceutical effects. Here, we developed a two-step model to evaluate the cellular immune response after SARS-CoV-2 infection-induced or spike protein stimulation in peripheral blood mononuclear cells (PBMC) from both unexposed and COVID-19 (primo-infected) individuals (Step1). Moreover, the supernatants of these cultures were used to evaluate its effects on lung cell lines (A549) (Step2). When PBMC from the unexposed were infected by SARS-CoV-2, cytotoxic natural killer and nonclassical monocytes expressing inflammatory cytokines genes were raised. The supernatant of these cells can induce apoptosis of A549 cells (mock vs. Step2 [mean]: 6.4% × 17.7%). Meanwhile, PBMCs from primo-infected presented their memory $CD4^+$ T cells activated with a high production of *IFNG* and antiviral genes. Supernatant from past COVID-19 subjects contributed to reduce apoptosis (mock vs. Step2 [ratio]: 7.2 × 1.4) and to elevate the antiviral activity (iNOS) of A549 cells (mock vs. Step2 [mean]: 31.5% × 55.7%). Our findings showed features of immune primary cells and lung cell lines response after SARS-CoV-2 or spike protein stimulation that can be used as an in vitro model to study the immunity effects after SARS-CoV-2 antigen exposure.

Keywords: in vitro model; immunity; SARS-CoV-2

1. Introduction

The infection caused by the new coronavirus (SARS-CoV-2) induces a severe acute respiratory syndrome, with signals and symptoms such as fever, cough, and pneumonia, namely COVID-19 [1,2]. This virus of high transmissibility and high mortality rates among respiratory infections has collapsed the intensive care units of hospitals around the world [1,2]. The only preventive measure to control the spread of this disease is vaccination combined with reducing social activities, wearing adequate masks, and hand sanitization [3–7]. As the SARS-CoV-2 variants were emerging in some parts of the globe, the pandemic showed its strength scaling up new cases and mortality rates, thus contributing to several countries joining in a race for mass immunization [3–7].

SARS-CoV-2 is a single-stranded, positive-stranded RNA virus between 60 and 140 nm in diameter with corona-like projections on its surface, formed by the spike glycoproteins (protein S), crucial for invading target cells [8]. Immune response is a key part of the clinical evolution of the disease, in which cytokine storm, leucopenia, and lung infiltrating macrophages and neutrophils are associated with poorer outcomes [2,9,10]. Nevertheless, some cellular immune responses during COVID-19 were described as crucial for host defense [2,11], where the main points are the heterogeneity of the immune system and potentially distinct patient immunotypes [12]. However, few studies are focused on Latin American countries, in which socio-economic issues are always challenging and genetic factors can influence different responses [13].

Viral reactivation and reinfection have been described and associated with successive contact with different SARS-CoV-2 strains [14–16]. In this way, memory phenotypes raised after infection should be more explored and compared with the phenotypes activated after vaccination [17–21]. Therefore, the function of immune response cells under live virus exposition is not well understood even in exposed or unexposed individuals to SARS-CoV-2 [22], and how the product of this cellular response can influence the pulmonary alveolar epithelial cells is not fully understood. Here, we developed an in vitro model to evaluate the events induced by live SARS-CoV-2 and spike protein in different subsets of immune in vitro cells (Step1), as well as the effects of these cellular immune response products in a lung cell line in the presence of SARS-CoV-2 (Step2). This two-step in vitro model provides useful information for a better understanding of the host interactions with SARS-CoV-2 and could guide future evaluation of vaccines and biopharmaceuticals.

2. Materials and Methods

2.1. Study Design

In this study, the goal is to present a two-step model to evaluate the cellular immune response against SARS-CoV-2 (whole virus) using in vitro cell cultivation carried out in a biosafety level III laboratory. The study was designed with the aim of investigating the cellular immune response using peripheral blood mononuclear cells (PBMC) from volunteers by antigenic stimulation, with spike protein and virus, as the first step (Step1). After that, the harvested supernatant from the immune cells was used in the cultivation of lung alveolar epithelial cells to evaluate antiviral/pathological effects of the cellular immune response, as the second step (Step2).

PBMC from naïve healthy volunteers and primo-infected COVID-19 individuals (without hospitalization), with one previous detection of SARS-CoV-2 by naso-oropharyngeal swabs RT-qPCR were submitted to cellular cultivation assay in the presence of live SARS-CoV-2 (infection-induced) and/or spike protein (antigen stimulation) [23]. PBMC were incubated for 48 h at 37 °C, in a humidified chamber, at 5% CO_2 and maintained with RPMI-1640 media as negative control (mock). Naive healthy volunteers are called unexposed from now on, and primo-infected COVID-19 individuals are called COVID-19 from now on (Tables 1 and 2).

Table 1. Clinical characteristics of the study population.

ID	Gender	RT-PCR SARS-CoV-2	Serology IgM/IgG	Signals & Symptoms	Age	Spike Assay (BSL2)	Virus Assay (BSL3)
1	F	Negative	Negative	No	45	Yes	No
2	M	Positive	Positive	Yes	44	Yes	Yes
3	F	Positive	Negative	Yes	28	Yes	No
4	F	Positive	Negative	Yes	38	Yes	No
5	F	Positive	Negative	Yes	37	Yes	No
6	M	Positive	Negative	Yes	29	Yes	No
7	M	Positive	Positive	Yes	28	Yes	No
8	F	Negative	Negative	No	32	Yes	No
9	F	Positive	Positive	Yes	32	Yes	Yes
10	F	Negative	Negative	No	29	Yes	No
11	M	Negative	Negative	No	31	Yes	No
12	M	Negative	Negative	No	45	Yes	Yes
13	F	Negative	Negative	No	42	Yes	Yes
14	F	Negative	Negative	No	31	Yes	Yes
15	F	Negative	Negative	No	52	Yes	No
16	F	Negative	Negative	No	39	Yes	Yes
17	M	Negative	Negative	No	26	Yes	No
18	M	Negative	Negative	No	24	Yes	No
19	F	Negative	Negative	No	28	Yes	Yes
20	F	Negative	Negative	No	30	Yes	No
21	F	Negative	Negative	No	36	Yes	Yes
22	M	Negative	Negative	No	38	Yes	Yes
23	M	Negative	Negative	No	38	Yes	Yes
24	M	Negative	Negative	No	31	Yes	Yes
25	M	Negative	Negative	No	29	Yes	Yes
26	F	Positive	Positive	Yes	34	Yes	Yes
27	M	Positive	Positive	Yes	56	Yes	Yes
28	F	Positive	Positive	Yes	58	Yes	Yes
29	M	Positive	Positive	Yes	34	Yes	Yes

The signal and symptoms reported by volunteers who had COVID-19 confirmed were fever, headache, myalgia, cough, and loss of smell/taste; each volunteer reported at least three of those symptoms. The duration of symptoms lasted up to two weeks. F: female, M: male. Descriptions about the assays performed in biosafety level II (BSL2) laboratory and biosafety level III (BSL3) laboratory. Blood draw was performed on May 2020.

Table 2. Descriptive frequencies of clinical characteristics.

		Unexposed (n = 18)	COVID-19 (n = 11)
RT-qPCR SARS-CoV-2	Positive	—	11 (100%)
	Negative	18 (100%)	—
Serology IgM/IgG	Positive	—	7 (63.6%)
	Negative	18 (100%)	4 (36.4%)
Signals and symptoms	Yes	—	11 (100%)
	No	18 (100%)	—
Demographic	Gender (F; M)	10; 8	6; 5
	Age (mean ± SD)	35 ± 8	38 ± 11

The protocol was performed with virus-infected or spike protein-stimulated PBMC (multiplicity of infection (MOI): 0.01 or 10 µg/mL for spike protein), as a control for viral antigen. Cells were tested by flow cytometry and gene expression (Step1). Human adenocarcinoma alveolar basal epithelial cells (A549-CCL-185) were cultured without and with the virus (MOI: 0.1), as well as with the resultant PBMC supernatants from Step1 to assess the effects of the soluble mediators from the cellular immune response in lung alveolar epithelial cells (Step2). All experiments were performed independently and in triplicates.

2.2. Samples

Blood samples were obtained from volunteers (n = 29, mean ± SE = 36 ± 1.9 years old, BMI < 30, 13 males) without SARS-CoV-2 infection at intake (RT-qPCR negative) (Table 1). Fifteen subjects showed no COVID-19 signals or symptoms and were negative for IgM/IgG SARS-CoV-2 antibodies. Three frozen samples were collected before the COVID-19 outbreak (June, July, and November 2019). Eleven subjects tested positive for SARS-CoV-2 infection by RT-qPCR according to the protocol described by Matos et al., 2020 [24] or IgM/IgG antibodies (>two–three months before blood collection), and all presented signals or symptoms of COVID-19. All volunteers were monitored weekly since March 2020, by RT-qPCR on naso-oropharyngeal swabs for SARS-CoV-2 detection [24] (Table 2).

SARS-CoV-2 strain was provided by Laboratório de Vírus Respiratório e do Sarampo, Instituto Oswaldo Cruz, Fiocruz (https://nextstrain.org/ncov: Brazil/RJ-314/2020 or GISAID #414045). It was not possible to confirm if the viral strain used in the experiments was the same that affected the volunteers, but in the meantime, six different strains of SARS-CoV-2 circulating in Brazil were reported [25]. Spike protein was provided by Laboratório de Engenharia de Cultivos Celulares (Lecc), Coppe/UFRJ. Cultivation assays using live virus were performed in a Biosafety Level III laboratory at FIOCRUZ. After viral inactivation using commercial reagents (from RNeasy Plus mini kit, Qiagen and Cytofix, BD Biosciences, San Diego, CA, USA), the final procedures of samples analysis and other experiments with cell cultivation were carried out in a Biosafety Level II laboratory at FIOCRUZ.

Ethical Statement

All procedures were performed according to the Helsinki Declaration for ethical procedures with registration number CAAE 34728920.4.0000.5262. All participants provided written informed consent (IRB# 34728920.4.0000.5262).

2.3. Laboratory Assays

2.3.1. Viral Detection by RT-qPCR

After 48 h of cell cultivation, 1×10^6 of live PBMC were harvested and centrifuged ($400\times g$, 5 min, 4 °C) in the presence or absence of the virus. PBMC and supernatant samples were used to extract viral RNA using RNeasy Plus Mini Kit (Qiagen) and submitted to RT-qPCR assay (Molecular Kit SARS-CoV-2 (E/RP), Bio-Manguinhos, Rio de Janeiro, Brazil) to detect SARS-CoV-2 genome as described by Matos et al., 2020 [24].

2.3.2. Step1: In Vitro Antigen-Specific Cellular Immune Response

To evaluate different subpopulations after infection, PBMC were harvested and washed in FACS buffer solution (2% fetal bovine serum in phosphate buffer solution, pH = 7.4). The cells were centrifuged at $400\times g$ for 10 min; the supernatant was collected and frozen at −70 °C. The cells' pellet was homogenized and then stained with live/dead cell viability dye (Thermo Fisher Scientific, L23105, Waltham, MA, USA) according to the manufacturer's protocol. The cells were washed in FACS buffer and stained with surface antibodies CD3-APC-Cy7, clone: SP34; CD4-PE, clone: RPA-T4; CD8-Brilliant Violet 605, clone: SK1; CD14-Brilliant Blue 700, clone: MOP9; CD16-FITC, clone: 3G8; CD56-PE-Cy5, clone: B159; HLA-DR-Brilliant Violet 650, clone: G46-6; CD69-Brilliant Violet 421, clone: FN50; CD95-PE-Cy7, clone: DX2; CD45RA-APC, clone: HI100; CCR7 (CD197) Brilliant Violet 510, clone: 3D12; CD19-PE-Cy5, clone: HD37. All from BD Biosciences, San Diego, CA, USA. After surface staining, cells were washed with FACS buffer and fixed (Cytofix, BD Biosciences, USA). To assess SARS-CoV-2 replication on PBMC, the antibodies to dsRNA were used (mouse monoclonal antibody (MAb) J2 Scion, Budapest, Hungary) [26]. The secondary antibody used to detect J2 (Mab) was chicken antimouse Alexa Fluor 488 (1:1000) purchased from Invitrogen (cat#A-21200, Waltham, MA, USA).

Intracellular staining (ICS) assay was also performed for cytokines detection to define subpopulations of $CD4^+$ and $CD8^+$ T cells after 48 h with spike protein stimulation. Stimulation was performed using 10 µL/mL anti-CD28/49d (BD Biosciences) and 10 µg/mL of spike protein (except for the unstimulated condition) in RPMI1640 medium at a final volume of 500 µL. Furthermore, 1× cell stimulation cocktail of PMA and ionomycin was used as a positive control (eBioscience). Cells were incubated for 48 h at 37 °C, and 1× protein transport inhibitor (eBioscience) was added in the last 4 h of incubation. At the end of incubation time, cells were washed and stained using a viability dye (Live/Dead Fixable Blue; Thermo Fisher Scientific) according to the manufacturer's protocol. Staining was carried out using the following surface antibodies as described above CD3-APC-Cy7, clone: SP34; CD4-PE, clone: RPA-T4; CD8-Brilliant Violet 605, clone: SK1; HLA-DR-Brilliant Violet 650, clone: G46-6; CD69-Brilliant Violet 421, clone: FN50; CD45RA-APC, clone: HI100; CCR7 (CD197) PE, clone: 3D12. After surface antigen staining, cells were washed twice in FACS buffer, and a fixation–permeabilization step was performed using the FOXP3 Transcription Factor Staining buffer set, according to the manufacturer's protocol (Ebioscience kit, cat#00-5523-00). The following antibodies were used for intracellular staining (IFN-γ BV510, clone: B27; IL-2 Brilliant Violet 421, clone: MQ1-17H12; IL-4 Brilliant Violet 711, clone: MP4-25D2; TNF PE-Cy7, clone: MAB11). All antibodies were purchased from BD Biosciences. Compensation beads (UltraCompeBeads, Invitrogen™, Carlsbad, CA, USA cat#01-2222-42; ArC™ Armine Reactive Compensation Bead kit, Invitrogen™, Carlsbad, CA, USA, cat#A10346) were used for compensation set-up. The unstimulated condition was used to subtract any background staining off the analysis. Positive ICS or after spike protein stimulation or virus infection was determined by detection of at least 10 SARS-CoV-2-specific T cells and a frequency of SARS-CoV-2-specific T cells of at least twice the corresponding unstimulated signal. Twenty-nine subjects were used for spike protein assay (n = 11 COVID-19 and n = 18 unexposed), and sixteen were enrolled for live virus assay (n = 6 COVID-19 and n = 10 unexposed) (Table 1).

All the steps were performed at 4 °C unless otherwise specified by the manufacturer. The acquisition was performed using LSR Fortessa flow cytometer (Becton Dickinson, San Diego, CA, USA), and data were analyzed using FlowJo™ software (Becton Dickinson). Gate strategy to analyze immune cells subpopulations and alveolar epithelial cells by flow cytometry is summarized in Figures 1–3, 5 and 7.

2.3.3. Cytokines/Chemokines Gene Expression

To evaluate the gene expression profile after challenge, same cellular RNA extracted for viral detection was quantified in spectrophotometer (Nanodrop Technologies, Waltham, MA, USA), followed by a complementary DNA (cDNA) synthesis from 250 ng of total RNA using the High-Capacity cDNA Reverse-Transcription Kit (Thermo Fisher Scientific), both procedures according to manufacturer's instructions. Analysis of gene expression was performed using Fluidigm (Biomark platform) assays, as described elsewhere [27].

Briefly, the software R Studio v. 3.4.0 custom scripts were used for parsing raw foreground and background intensities, exported from the commercial Fluidigm® software. Fluorescence accumulation and melting curve graphs of Rn for each reaction with each gene were inspected. For quantification of relative gene expression, the fluorescence accumulation data of each sample were used for fitting four-parameter sigmoid curves using the 'qpcR' v. 1.4.1 R package. For each gene, efficiency was estimated by the mean of all efficiencies. Reference genes *18S*, *GAPDH* and *RPL13* were chosen based on stability measure from geNorm method. Sample-wise normalization factors were calculated by taking the geometric average of selected reference genes [28,29].

2.3.4. Step2: Human Alveolar Lung Epithelial Cells (A549) Cultivation with Supernatant from PBMC Cultured with SARS-CoV-2

Infected (MOI:0.1) and noninfected A549 cells (ATCC-CCL-185) 5×10^5/well were cultured in a 24-well plate for 48 h at 37 °C, in a humidified chamber, at 5% CO_2 with a pool of defrost supernatant from PBMC cultivated with live SARS-CoV-2 particles, from

Step1. A549 cells were harvested to evaluate the expression of nitric oxide synthase (iNOS) (iNOS/NOS2-FITC, cat#610331, BD Biosciences) and caspase-3 (VP-C308, Vector Labs) expression in lung cells by flow cytometry. The dsRNA staining was performed to detect the percentage of virally infected A549 cells, as previously described for PBMC samples (item 2.3.2). The secondary antibody used to detect caspase-3 and dsRNA was chicken antimouse Alexa Fluor 647 (1:1000) purchased from Invitrogen (cat#A-21463, Waltham, MA, USA). The viral infection on A549 cells was performed to distinguish the effects induced by the virus and/or by the products of cellular immune responses.

2.4. Statistical Analysis

The normality assumption of the data was initially evaluated by the Kolmogorov–Smirnov test or Shapiro–Wilk. Differences between groups were assessed using the Mann–Whitney *t* test, considering the investigation groups. Bar graphs are represented as mean ± standard error (SE). The software GraphPad Prism for Macintosh, version 8.4.2 (San Diego, CA, USA) was used to perform statistical analysis. The significance for all statistical analyses was defined as $p < 0.05$.

Baseline signals of activated cells in unstimulated controls were subtracted from SARS-CoV-2-stimulated assays to enable the visualization of SARS-CoV-2-induced or SARS-CoV-2-specific cell signals. Cell frequencies above one percent were considered for the final analysis.

3. Results

3.1. SARS-CoV-2 Replication on Mononuclear Cells Subsets

The first analysis was aimed at investigating the presence of SARS-CoV-2 replication inside the peripheral blood mononuclear cells. All blood samples were negative for SARS-CoV-2 RNA by qPCR before infection of the cell culture. The replicative dsRNA as well as significative viral loads in supernatants were detected after 48 h of virus exposure of PBMCs from all individuals (Figure 1b).

Overall, the analysis of absolute frequency of phenotypes before stimulation showed that lymphocytes (T and B cells) were more frequent than monocytes and natural killer cells in the peripheral blood cells from all participants, showing no difference between unexposed and COVID-19 groups (Table 3).

Table 3. Absolute frequency of circulating peripheral blood mononuclear cells from the study population.

	Unexposed (Mean ± SE)	COVID-19 (Mean ± SE)	*p* Value
T cells	36.75 ± 4.03	30.7 ± 3.00	0.48
B cells	15.25 ± 4.75	8.48 ± 3.38	0.22
Monocytes	2.73 ± 1.68	3.31 ± 1.55	0.25
Natural killer	1.61 ± 0.45	1.34 ± 0.27	0.11

Data of the absolute frequency from PBMC are expressed as percentage (%). The identification of the cell phenotypes were according to the gate strategy described in Figure 1a. SE: standard error.

The viral replication (dsRNA) was found in all cellular phenotypes explored, as monocytes, lymphocytes T and B, and natural killer cells. Our data show that viral SARS-CoV-2 infectivity in PBMC was similar for COVID-19 and unexposed subjects (Figure 1a,b).

3.2. Step1: SARS-CoV-2 Effects on the Functionality of PBMC Phenotypes and Cytokine Gene Expression

No changes in live cells percentages using PBMC from unexposed and COVID-19 were detected after in vitro spike protein exposure (Figure 1). However, a strong reduction of total live monocytes was observed (Figure 1e) in the evaluation of phenotypes after virus exposition (mock vs. virus (mean): unexposed: 55.4% × 23.9%, $p < 0.0001$; COVID-19: 48.2% × 11.0%, $p < 0.0001$).

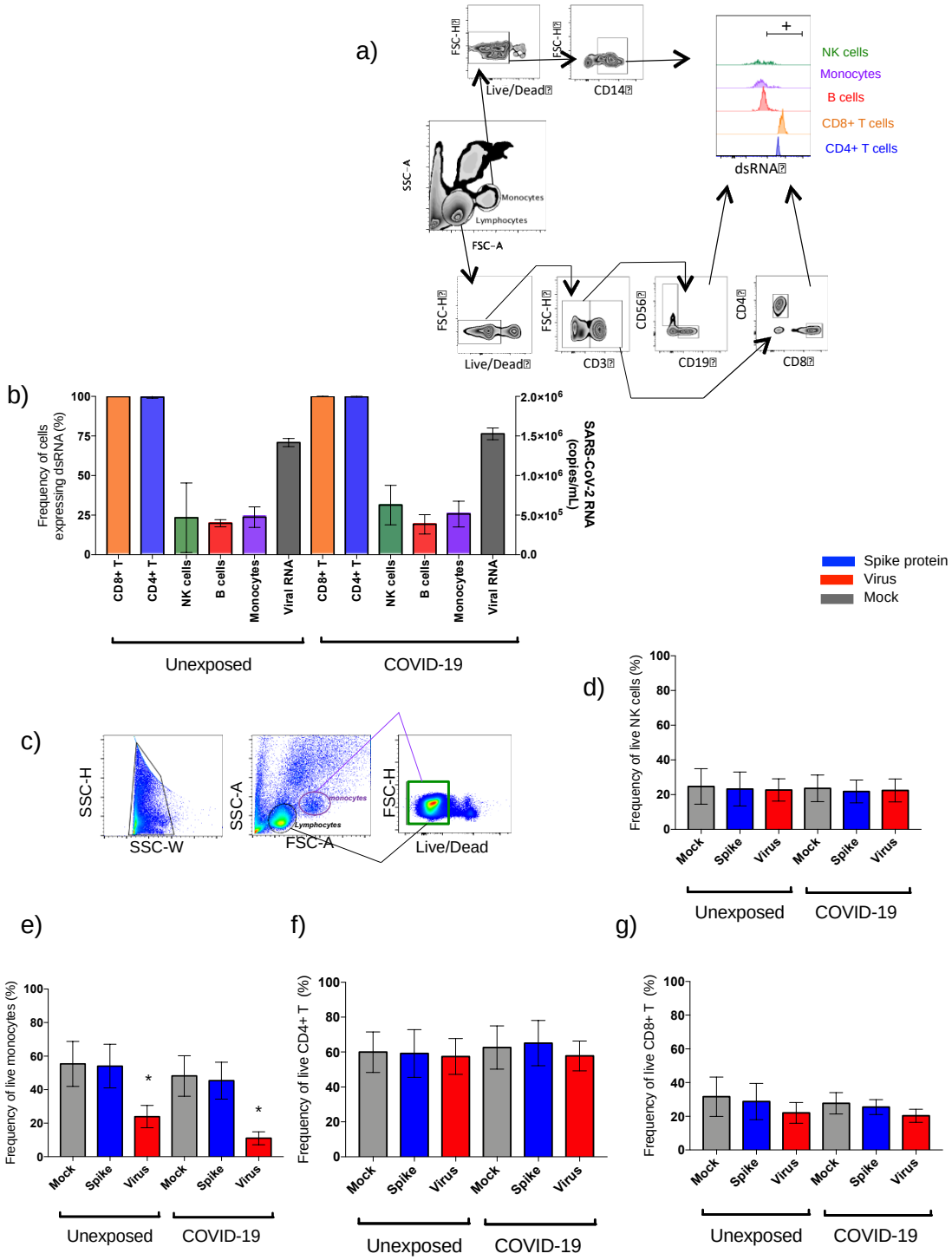

Figure 1. Presence of SARS-CoV-2 in PBMC and the percentage of live phenotypes exposed to spike protein and to live SARS-CoV-2. Gate strategy to get the subpopulations evaluated. (**a**). Viral load of RNA detected on supernatant from unexposed and COVID-19 PBMC cultured with live virus and frequency of double-strand (ds) RNA detection in different phenotypes, as $CD8^+$T, $CD4^+$T, natural killer (NK), B lymphocytes, and monocytes after in vitro cultivation (**b**). Gate to define total live PBMCs are represented with green lines (FSC-H vs. Live/Dead) with lymphocytes in black and monocytes in purple on the backgating (**c**). Subsequently, to separate natural killer from $CD4^+$ and $CD8^+$ T cells, we used CD56 marker to natural killer, and CD3 marker to define the T-cells subpopulation. Data from PBMC cultured with spike protein (blue) and SARS-CoV-2 (red) on total live natural killer (NK: $CD56^+CD3^-$) (**d**), total live monocytes (**e**), and total live T lymphocytes ($CD3^+CD4^+$) (**f**) and ($CD3^+CD8^+$) (**g**). The data are representative of 2–5 different experiments. * $p < 0.05$, ** $p < 0.01$, and *** $p < 0.001$.

3.2.1. Natural Killer Cells

Regarding subsets of SARS-CoV-2-infected natural killer cells, significant differences were documented for unexposed and COVID-19 (Figure 2a–c and Figure 4a,f). Natural killer subsets (NK^{bright} [$CD56^{high}CD16^{low}CD3^{-}$] and NK^{dim} [$CD56^{low}CD16^{high}CD3^{-}$]) showed a significant increase in their percentage after virus infection in unexposed individuals, while the same result was not observed for COVID-19 (Figure 2a–c). In addition, NK^{dim} ($CD56^{low}CD16^{high}CD3^{-}$) frequencies were significantly higher in unexposed than COVID-19 after contact with live SARS-CoV-2 (Figure 4a,f). In contrast, after spike protein stimulation, no differences in NK subsets percentages were observed (Figure 2a–c and Figure 4a,f).

3.2.2. Monocytes

Classical ($CD14^{+}CD16^{-}$) and intermediate ($CD14^{+}CD16^{+}$) monocytes percentages decreased significantly after in vitro SARS-CoV-2 infection-induced in all subjects (Figure 2d–f). Unexposed subjects presented a significant increase (Figure 2d–f), and the highest percentages of nonclassical monocytes compared to COVID-19 (Figure 4b,f). In contrast, no changes were observed in monocytes subsets percentages after spike protein stimulation (Figure 2d–f and Figure 4b,f).

3.2.3. $CD4^{+}$ T and $CD8^{+}$ T Lymphocytes

Upon spike protein stimulation or SARS-CoV-2-infection, $CD4^{+}$ T and $CD8^{+}$ T cells showed particular features considering the nature of exposition while unexposed, and COVID-19 could represent the first and second virus exposure, respectively, using the in vitro assay (Figures 3–5).

$CD4^{+}$ T cell percentage was ~10-fold low compared to CD8+ T cells based on the evaluation of the early activation marker, CD69, together with HLA-DR (marker of cellular activation) after viral infection in both groups of individuals (Figures 3a–c and 4c,d). Spike protein from SARS-CoV-2 showed to be a good T-cell stimulation for COVID-19 (Figures 3b,c and 4c,d,f), with high production of IFN-γ, IL-2, and TNF by $CD4^{+}$ T cells, characterizing the predominant response of Th1 cells. In the COVID-19, Th1 cells were significantly higher than Th2 $CD4^{+}$ T cells, which produced IL-4, IL-2, and TNF, main markers for Th2 response (Figure 3d).

Spike-stimulated PBMCs exhibited high $CD8^{+}$ T-cell frequencies, with IFN-γ, IL-2, and TNF production in COVID-19 (Figure 3d). By contrast, SARS-CoV-2-infected PBMCs showed lower levels of activated $CD8^{+}$ T cells in COVID-19 compared to the unexposed group (Figure 4d).

The apoptotic marker, CD95, was elevated independently of previous disease in $CD4^{+}$ T and $CD8^{+}$ T cells after SARS-CoV-2 infection (Figure 3e,f). However, apoptotic $CD8^{+}$ T cells ($CD95^{+}$) were significantly higher in COVID-19 than unexposed individuals (Figures 3e,f and 4e,f). Meanwhile, spike protein showed no changes for apoptotic T cells (Figures 3e,f and 4e,f).

3.2.4. Memory T Lymphocytes

Memory phenotype of T cells was explored to explain differences among naive and primed T cells. Figure 5 displays analysis of memory phenotypes as central memory (CM: $CD45RA^{-}CCR7^{+}$), effector memory (EM: $CD45RA^{-}CCR7^{-}$), naïve cells (naïve: $CD45RA^{+}CCR7^{+}$), and terminally differentiated (TEMRA: $CD45RA^{+}CCR7^{-}$). We observed that unexposed individuals were predominantly naïve either for virus or for spike protein as expected, therefore validating our model (Figure 5).

After spike stimulation, a significant elevation for central and effector memory $CD4^{+}$ T-cells frequencies was detected for COVID-19, followed by all memory subsets for $CD8^{+}$ T cells, except for naive subset, compared to the unexposed group (Figure 5a–e,g). After SARS-CoV-2 infection, the only alteration on the memory T cells was on the frequency of

central memory CD4⁺ T cells, also higher in the COVID-19 as compared to the unexposed group (Figure 5f,h).

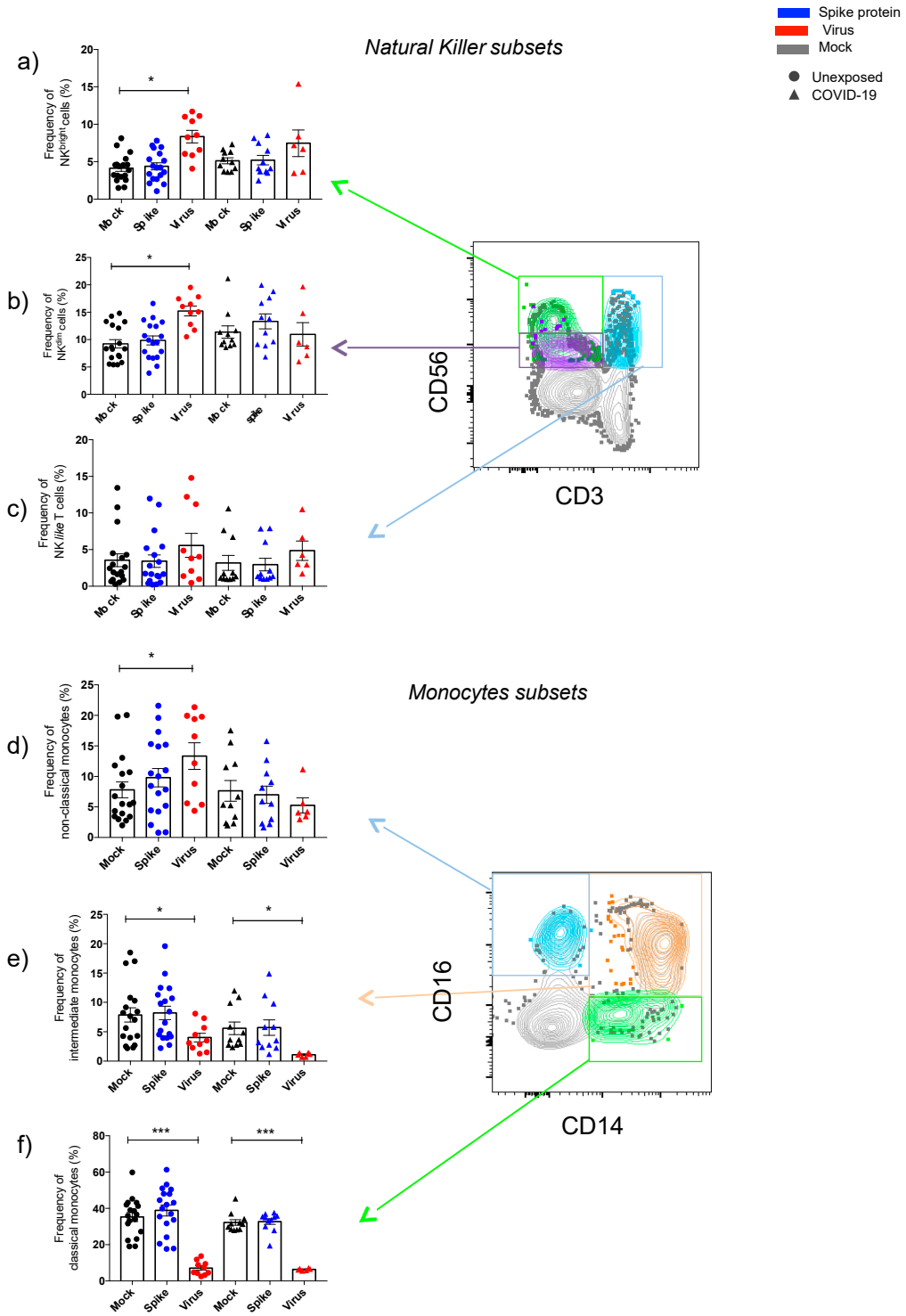

Figure 2. Effects of SARS-CoV-2 on natural killer and monocytes subsets. The percentage of natural killer (NK) subsets are displayed for NK^{bright} ($CD3^{-}CD56^{high}CD16^{low}$) (**a**: green color in the dot plot), NK^{dim} ($CD3^{-}CD56^{low}CD16^{high}$) (**b**: purple), and NK-like T cells ($CD3^{+}CD56^{+}$) (**c**: blue) in both groups, unexposed and SARS-CoV-2 exposed (COVID-19), up to 48 h of cell cultivation in the presence of spike protein and live SARS-CoV-2. The percentage for monocytes subsets were divided in nonclassical monocytes ($CD14^{-}CD16^{+}$) (**d**: blue color), intermediate monocytes ($CD14^{+}CD16^{+}$) (**e**: orange color), and classical monocytes ($CD14^{++}CD16^{-}$) (**f**: green) on cell cultivation with antigens. The data are representative of 2–5 different experiments. * $p < 0.05$, ** $p < 0.01$, *** $p < 0.001$.

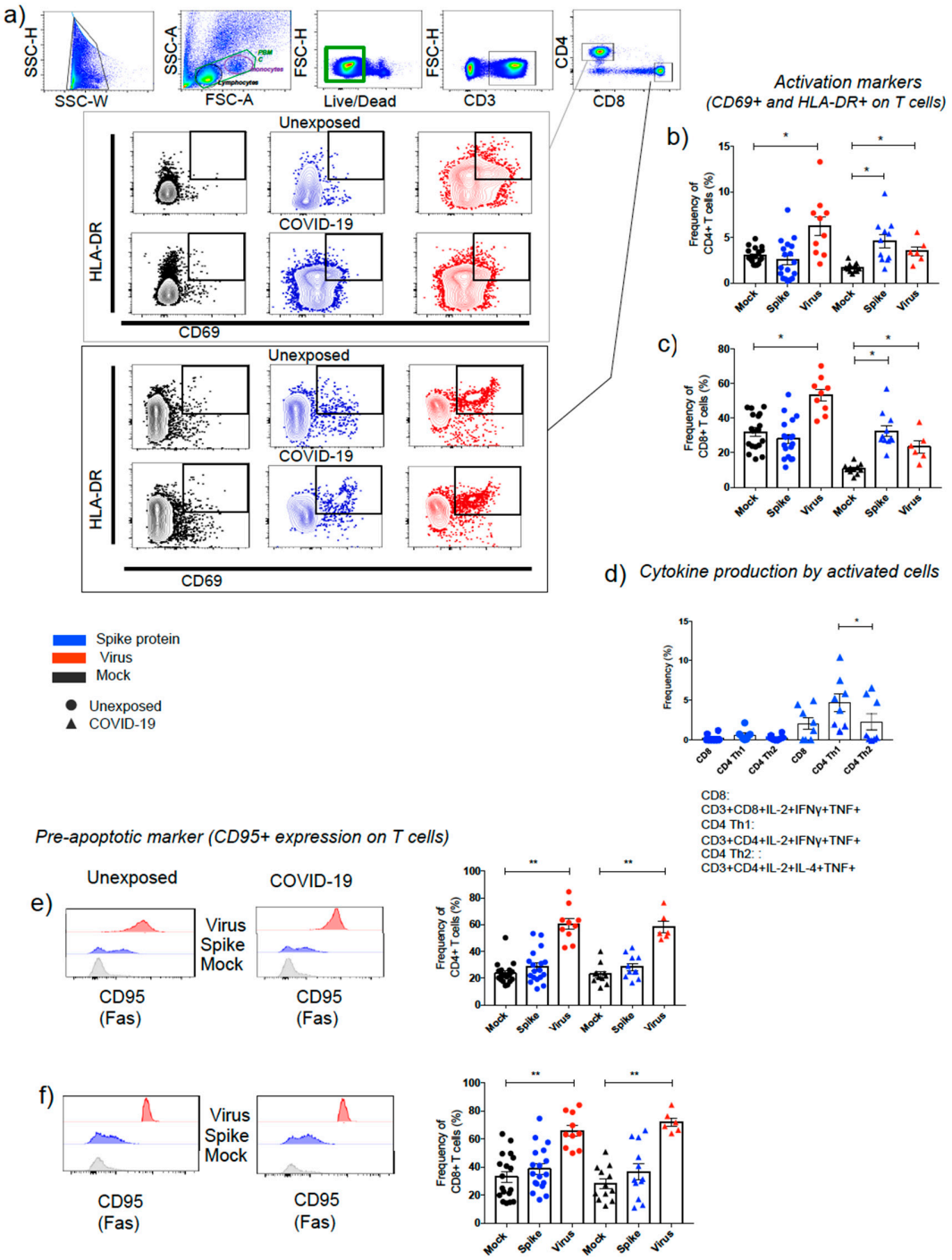

Figure 3. SARS-CoV-2 effects on lymphocytes T activation and pre-apoptosis. Gate strategy to define the subpopulations using dot plot FSC vs. SSC (green dashed line represents PBMC, purple line is the monocytes, and black line is the representation of lymphocytes. Gate to define total live PBMCs are represented with green line (FSC-H vs. Live/Dead). After gating live $CD3^+$ T cells, it was possible to set activated T cells ($CD4^+$ and $CD8^+$), showing nonstimulated (black), stimulated with spike protein from SARS-CoV-2 (blue), and exposed with live virus (red) (**a**). Percentages obtained from unexposed and COVID-19 displaying data for $CD4^+$ (**b**) and $CD8^+$T cells (**c**) activated by antigens. The intracellular staining assays with spike protein is showing $CD8^+$ T lymphocytes producing IL-2, TNF and IFN-gamma, as well as $CD4^+$ subsets, $CD4^+$ Th1 and $CD4^+$ Th2 with their main representative cytokines production by those cells in both groups, unexposed and SARS-CoV-2 exposed (COVID-19) (**d**). The expression of pre-apoptotic marker ($CD95^+$) on $CD4^+$ (**e**) and on $CD8^+$ T cells (**f**) is displayed. The data are representative of 2–5 different experiments. * $p < 0.05$, ** $p < 0.01$, and *** $p < 0.001$.

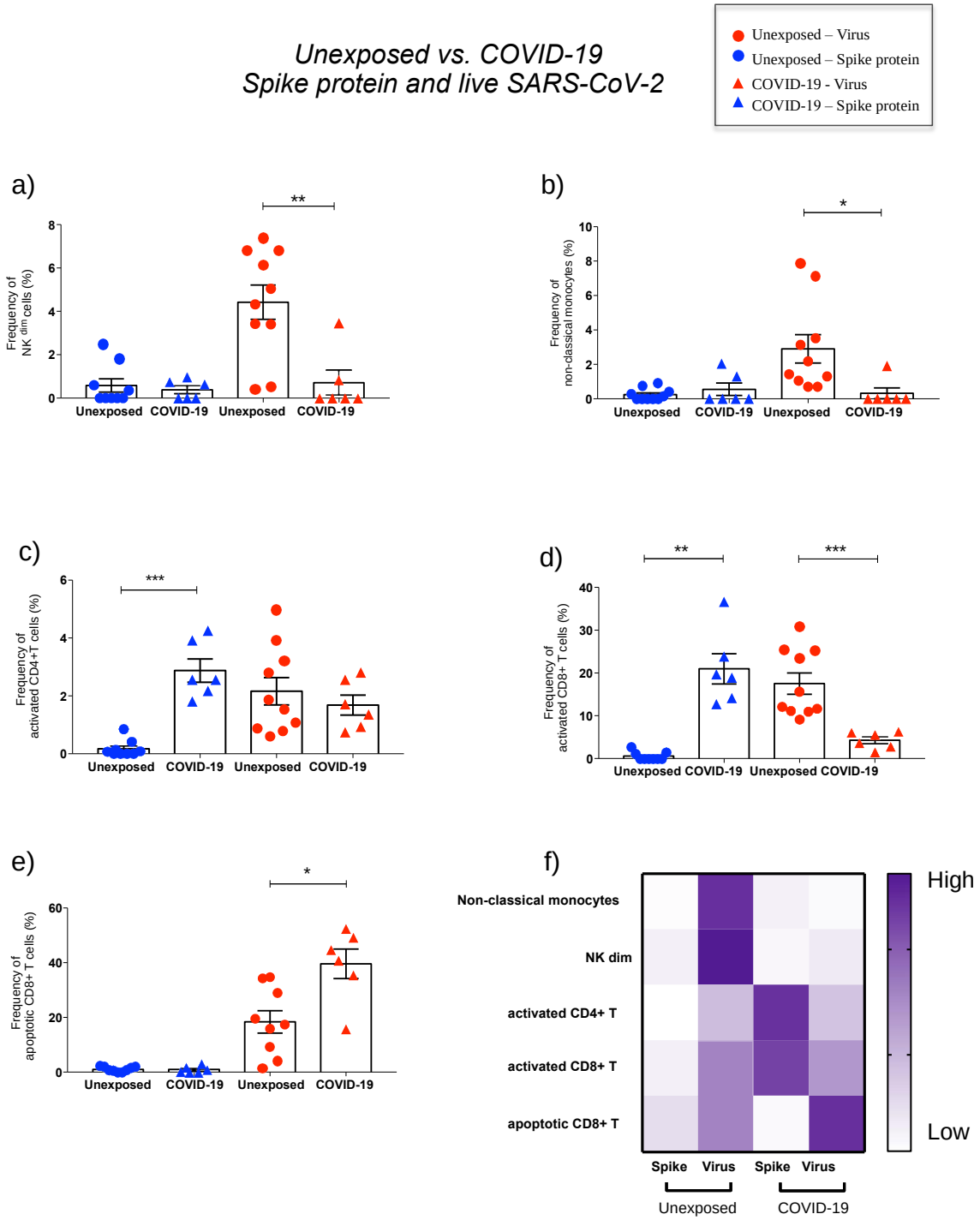

Figure 4. Major effects of spike protein and live SARS-CoV-2 on PBMC phenotypes comparing unexposed and COVID-19 groups. Percentage of natural killer cytotoxic subset (NK^{dim}, $CD3^{-}CD56^{low}CD16^{high}$) (**a**) and nonclassical monocytes ($CD3^{-}CD14^{-}CD16^{+}$) (**b**) in unexposed (circles) and COVID-19 (triangles) after spike protein (blue) and in vitro virus exposure (red). Percentage of activated ($CD69^{+}HLA-DR^{+}$) $CD4^{+}$ (**c**) and $CD8^{+}$T lymphocytes (**d**), as well as apoptotic ($CD95^{+}$) $CD8^{+}$ T lymphocytes (**e**) after antigen stimulation (spike protein and virus). Heat map of phenotypes percentages affected by spike protein and live virus stimulation on unexposed and COVID-19 (**f**). The final value percentage represented by *y* axis is the percentage of cells activated by SARS-CoV-2 antigens subtracted from unstimulated cells (% of cells stimulated with spike protein or virus minus % of the cells from mock condition). Symbols legend represents each sample collected from each volunteer. The data are representative of 2–5 different experiments. * $p < 0.05$, ** $p < 0.01$, and *** $p < 0.001$.

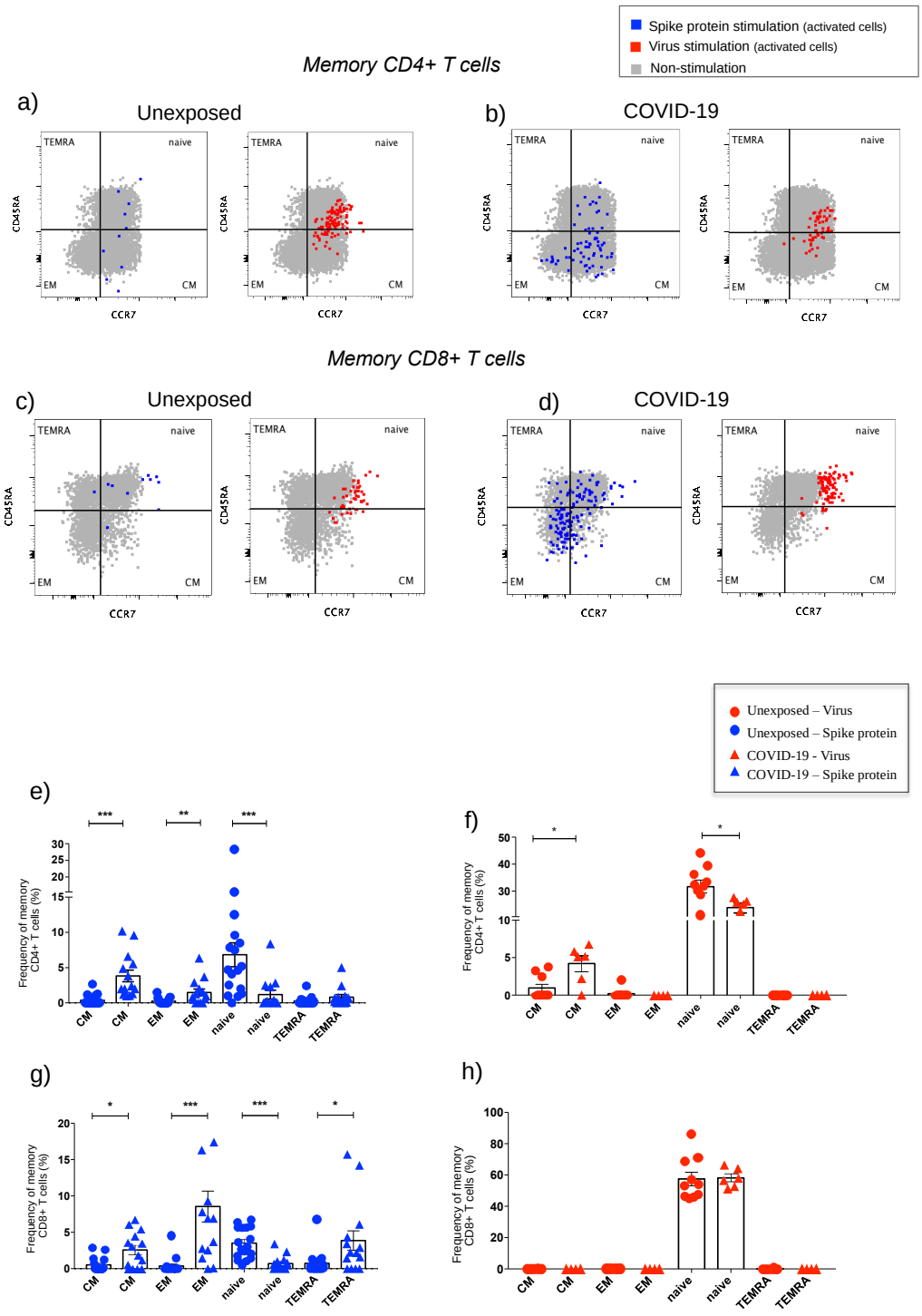

Figure 5. Memory T-cells phenotypes affected by spike protein stimulation and by live SARS-CoV-2 exposure. Percentages of memory T-cells phenotypes, as central memory (CM: $CD45RA^{-}CCR7^{+}$), effector memory (EM: $CD45RA^{-}CCR7^{-}$), naïve cells (naïve: $CD45RA^{+}CCR7^{+}$), and terminally differentiated (TEMRA: $CD45RA^{+}CCR7^{-}$) are represented (**a**–**h**). Total of memory T cells are in grey color (bulk: without antigen stimulation), and activated phenotype cells ($CD69^{+}HLADR^{+}$) are represented in blue for spike protein stimulation and in red for live virus in dot plot graphs (**a**–**d**). The memory $CD4^{+}$ T (**e**,**f**) and $CD8^{+}$ T cells (**g**,**h**) percentages from unexposed and COVID-19 are displayed by bar graphs. The final percentage value, represented by *y* axis, is the percentage of cells activated by SARS-CoV-2 antigens subtracted from unstimulated cells (% of cells stimulated with spike protein or virus minus % of the cells from mock condition). The data are representative of 2–5 different experiments. Symbols legend represents each sample collected from each volunteer. * $p < 0.05$, ** $p < 0.01$, and *** $p < 0.001$.

3.2.5. Expression of SARS-CoV-2 Response Genes

Subsequently, we evaluated gene expression patterns associated with biological processes such as virus entry, apoptosis, inflammation, and general innate antiviral response. A slight increase in the frequency of innate cells in the unexposed group was detected. SARS-CoV-2-infected PBMC from COVID-19 presented a significantly higher expression of genes related to virus entry (cellular SARS-CoV-2 receptor *ACE2*) and apoptosis (*CARD6*, and *CARD9*); reinforcing $CD8^+$ T cells $CD95^+$ immunophenotyping (Figure 6a,b). In addition, our data showed that second exposure to the virus leads to a more intense inflammatory process with higher levels of proinflammatory *CCL4*, *CCL5*, *CXCL10*, *TNF*, and *NRPL3*, together with regulators *IL10* and *TGFB* (Figure 6c,d). Moreover, COVID-19 presented a robust antiviral response including higher levels of *IFNG*, a hallmark of $CD8^+$ T cells activity and $CD4^+$ T cells Th1 response, type I interferons (*IFNA* and *IFNB*) and their receptors (*IFNAR1*), transcriptional regulators (*STAT2*, *IRF3*, *IRF7*, and *IRF9*) and interferon-stimulated genes (*OAS2*, *OAS3*, *ISG15*, *RNASEL*, *IFIT5*, and *RIGI*) (Figure 6e).

Spike COVID-19 protein stimulation also leads to increased gene expression of *CARD9*, and *CCL5* (Figure 6b,c). A remarkable increase for genes related to interferon response was observed (*IFNA*, *IFNG*, *IRF3*, *OAS1*, *OAS2*, *ISG15*, *RNASEL*, *IFIT5*, and *RIGI*), in contrast with the unexposed group (Figure 6e).

3.3. Step2: Effects of Supernatant from PBMC Cell Cultivation in Lung Alveolar Epithelial Cells

The supernatant from SARS-CoV-2-infected PBMCs was used as a conditioned medium to evaluate the interaction among soluble mediators of immune response and lung alveolar epithelial cells (A549). The replication of SARS-CoV-2 on A549 cells was measured by dsRNA staining, in which infected A549 cells expressed dsRNA, as expected (Table 4). A slight decrease in dsRNA expression was observed comparing A549 infected and A549 noninfected cells in the presence of supernatant derived from PBMC virus exposition for both groups, unexposed and COVID-19, but not significant (Table 4).

Table 4. Frequency of A549 cells (%) expressing dsRNA.

	Infected	**Noninfected**	***p* Value Infected vs. Noninfected**
Mock A549	56.34 ± 3.34	1.47 ± 0.32	0.018
NC (Unexposed)	57.82 ± 1.25	1.48 ± 0.43	0.019
NC (COVID-19)	53.71 ± 8.32	1.40 ± 0.33	0.024
Virus (Unexposed)	54.32 ± 6.43	42.2 ± 7.31	0.221
Virus (COVID-19)	55.61 ± 7.82	42.3 ± 9.60	0.250

Data are represented by mean ± SE. NC: negative control, as supernatant from mock condition of PBMC cultivation.

The antiviral defense activation evaluation by nitric oxide synthase expression (iNOS), as well as the apoptotic effect (caspase-3 expression) of PBMCs supernatants in A549 cells, infected or not, was performed (Figure 7). Cellular responses from unexposed individuals did not change the iNOS expression by A549 (Figure 7b,f), even after SARS-CoV-2 infection of the alveolar epithelial cells (Figure 7d,f). On the other hand, the caspase-3 expressed by A549 frequencies was elevated after PBMC supernatant from unexposed subjects compared to COVID-19 (Figure 7c,e).

The contact with the live virus by PBMC from primo-infected subjects displayed a significant elevation of A549 expressing iNOS, as well as a reduction of caspase-3 by those cells before SARS-CoV-2 infection compared to the unexposed group (Figure 7b,c). After viral infection of alveolar epithelial cells, the product of cellular immune responses from COVID-19 remained inducing the reduction of caspase-3 expression by A549 cells (Figure 7e,g).

Figure 6. Normalized gene expression of peripheral blood mononuclear subset cells from individuals exposed to SARS-CoV-2 or otherwise after stimuli with spike SARS-CoV-2 protein. Detailed scatted dot plots show normalized expression for genes analyzed in COVID-19 (triangular shapes) or unexposed individuals (circular shape), according to experimental stimuli with spike protein (blue dots) or SARS-CoV-2 (red dots). The number of dots varies according to gene analyzed due to failed amplifications. Boxes represent the median and vertical bars as well as the standard error of normalized expression for each experimental group analyzed using references genes RPL13 and 18S. Genes were clustered in boxes according to biological/immunological functions: SARS-CoV-2 receptors (black) (**a**), apoptosis (purple) (**b**), inflammation (red) (**c**), regulation of inflammation (green) (**d**), and innate antiviral response (blue) (**e**). Graphics and statistical comparisons of normalized expression for unexposed and COVID-19 using Mann–Whitney test in software GraphPad Prism 8.4.2. * $p < 0.05$, ** $p < 0.01$, and *** $p < 0.001$.

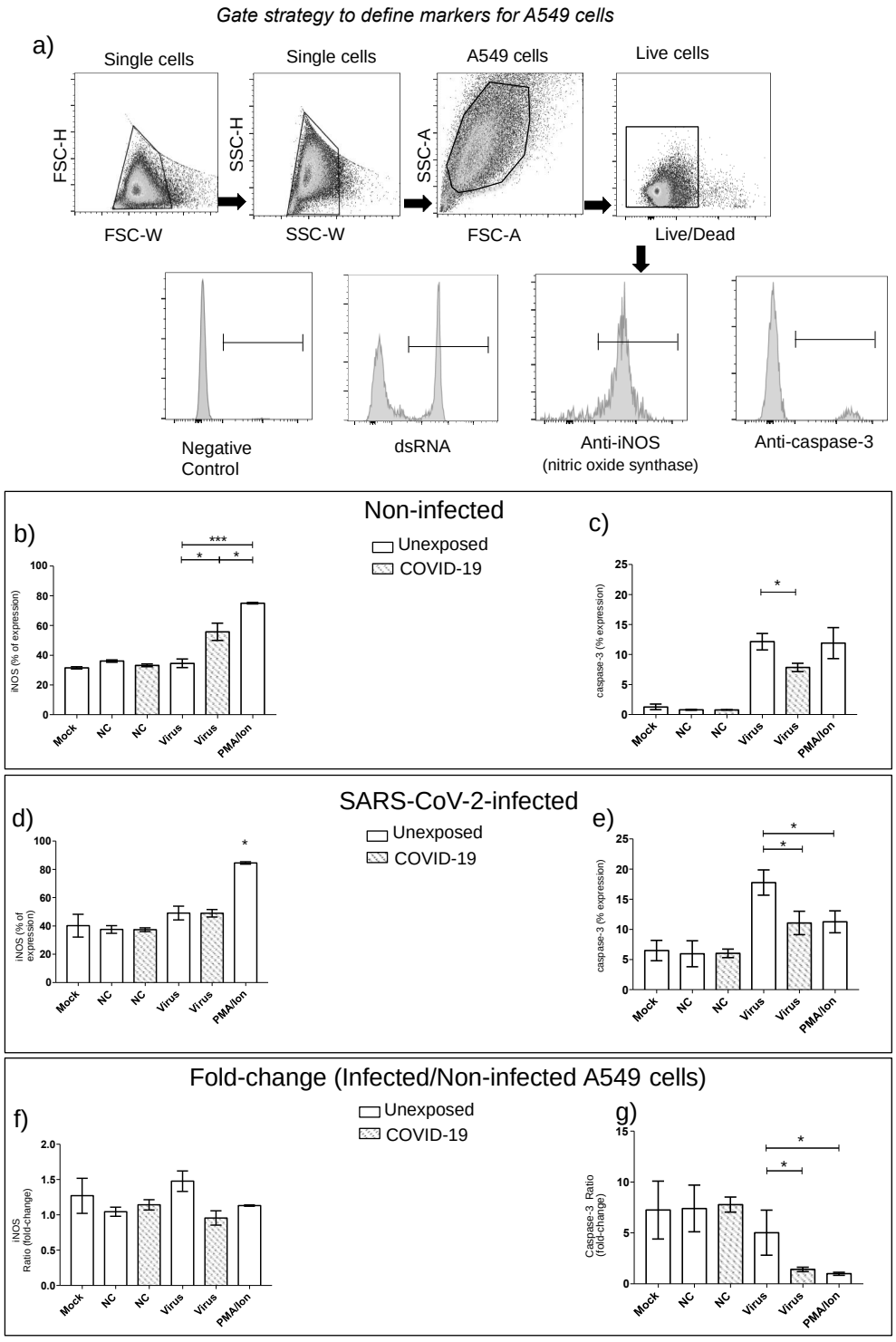

Figure 7. Effects of supernatant from PBMC cell cultivation on lung alveolar epithelial cells. A549 cell data of nitric oxide synthase (iNOS), double-strand RNA (dsRNA), and caspase-3 expression evaluation (**a**). Data from the supernatant from unexposed and COVID-19 PBMC cultivation with live SARS-CoV-2 expressing iNOS (**b**) and caspase-3 (**c**) in A549 noninfected cells. Data from the A549 cells expressing iNOS (**d**) and caspase-3 (**e**) after 48 h of SARS-CoV-2 infection. The fold-change (infected/noninfected) of iNOS (**f**) and caspase-3 (**g**) expression by A549 cells. The supernatant pool from unexposed and COVID-19 PBMC on incubation with SARS-CoV-2 was used. PMA/Ion: Supernatant from proliferative T-cell responses stimulated by polyclonal activator. NC- supernatant from negative control used in the antigen-stimulation assay. The data are representative of 2–5 different experiments. * $p < 0.05$, ** $p < 0.01$, and *** $p < 0.001$.

4. Discussion

Several studies have already demonstrated that the new coronavirus (SARS-CoV-2) is able to infect not only cells in the respiratory tract, but other organs, such as blood [30–33]. Our findings showed that peripheral blood mononuclear cells, such as B and T lymphocytes, monocytes, and natural killer cells, can be infected by SARS-CoV-2. Pontelli et al. (2020) [13] found the SARS-CoV-2 replication on the same cells explored here, but not for natural killer cells subsets. Meanwhile, some studies supported the decrease in NK cells frequencies in peripheral blood [34], and their inflammatory function on the pulmonary tract in post-mortem COVID-19 cases [35]. Intriguingly, our results for the natural killer cells displayed a high percentage of cytotoxic phenotype (NK^{dim}) in unexposed individuals, thus corroborating their activation by viral proteins similarly observed at NK derived from peripheral blood of COVID-19 patients [36].

Monocytes percentages were reduced after in vitro virus exposure and in severe COVID-19 cases, as described by others [37,38]. Nevertheless, a slight increase in nonclassical monocytes ($CD14^{-}CD16^{+}$) was observed in the unexposed group after SARS-CoV-2 contact, which may be induced by viral proteins, as noted in the blood of patients with moderate COVID-19 compared to controls (unexposed subjects) [37].

Natural killer cells are the main cell type related to proinflammatory cytokines production at the first line of immune defense against viruses, and it seems to be involved with monocytes/macrophages in the cytokine storm observed in COVID-19 patients [10,34]. Cytokines produced in this context by NKs and monocytes might be the key in severity, while inhibition of TNF, CXCL8, and IL6 have been identified as possible therapeutic targets [39]. In this regard, our results demonstrated a considerable enhancement of inflammatory mediators in SARS-CoV-2-infected PBMCs from unexposed volunteers related to monocytes and NK cells activation. The global decrease in monocyte percentages observed in our model suggests a nonsustained inflammatory response [40].

Lymphocyte T percentages have been measured as an indicator of severity for COVID-19 outcomes, such as lymphopenia; exhaustion and apoptosis of T cells were noted in COVID-19 patients [41–46]. We observed here that all participants showed a high expression of the apoptotic marker CD95 after virus infection (Fas), detected mainly in $CD8^{+}$ T cells. Moreover, there is a consistent correlation between lymphopenia and prognosis [41–46]. In addition, histopathological analysis of lungs of post-mortem patients showed an important infiltration by T lymphocytes [47,48].

SARS-CoV-2 proteins have been associated with T-cell activation and memory phenotypes after COVID-19 recovery [46,49–53]. B- and T-cell responses are detected in the blood around 1 week after the onset of symptoms. Regarding the general cell response, we present the following findings: autopsies of patients with COVID-19 revealed increased cell exhaustion and SARS-CoV-2 $CD4^{+}$ expressing IFN-γ, TNF-alpha, and IL-2 indicating a Th1 cellular response [54]. After two weeks of symptoms, cellular phenotypes that have specific memory T cells for SARS-CoV-2 in peripheral blood begin to appear. This process can provide useful information on cellular protective/lasting immunity [55].

Considering the previous exposure to SARS-CoV-2, our data demonstrated that T cells from unexposed individuals are not able to recognize the spike protein, but the virus infection was capable of inducing a robust T cell activation in unexposed similar to the clinical findings [46,49–53].

$CD4^{+}$ T helper has been implicated in the pathogenesis that leads to the inflammation process, as well as being affected by SARS-CoV-2 replication, diminishing the T follicular helper cells, contributing to the loss of antibodies, and reduction of IFN-γ production in COVID-19 patients [35,46,49–53,56]. Our findings showed that spike viral protein led to the activation of $CD8^{+}$ T and $CD4^{+}$ T helper cells producing IFN-γ (Th1), and expression of genes related to interferon pathways in COVID-19 individuals.

Additionally, ex vivo studies with COVID-19 patients showed that reactive $CD4^{+}$ T cells are able to produce high levels of chemokines [49,57–59]. Here, we also demonstrated that PBMC from primo-infected individuals after virus infection presented a higher antivi-

ral response including high expression of *IFNG*, a key to Th1 differentiation [60] and $CD8^+$ T cell activation [61]. Taken together, these results also suggest that $CD4^+$ T cells from COVID-19 could be key players on inflammatory and antiviral responses upon a second exposition, which would be advantageous for the vaccines.

Concerning the memory T cell phenotypes, our results showed that unexposed individuals only have naïve T cells raised after antigen stimulation, as described for viral infections or vaccination [62–64] and differently as noted by others [52,53]. Our data corroborate the findings described by Grifoni et al. (2020) [53] about central memory $CD4^+$ T-cell activation in subjects recovered from mild COVID-19 infection after stimuli with viral proteins. Moreover, this scenario is expected as a good signal of positive response for vaccines, in which the next contact with a viral protein, or whole virus, could promote T-cell recognition, activation, and consequently full protection with *IFNG* gene expression and IFN-γ production by $CD4^+$ T cells [53,55,65].

In the pathway to investigate the output of cellular responses on the alveolar epithelial lung cells (A549) after in vitro exposure to SARS-CoV-2 antigens, the nitric oxide synthase (iNOS) and caspase-3 expression by A549 were assessed aiming at evaluating if their expression can be regulated by cytokines among other mediators produced by infected cells [66–70]. The antiviral activity in supernatants provided alterations in the alveolar epithelial lung cells (A549) during our in vitro assay. Despite no changes of viral replication (dsRNA), the consequences were the reduction of caspase-3 expression in SARS-CoV-2 infected cells and elevation of iNOS expression in noninfected A549 cells. Probably, the cellular immune response may help towards the antiviral activity and could raise the nitric oxide (NO) production by A549 cells, a product of iNOS function, described to be effective in reducing SARS-CoV-2 replication in patients with COVID-19 [71,72]. However, further investigations are needed to better understand the role and complexity of the immune response after SARS-CoV-2 exposure, even for COVID-19.

It is worth noting that our data need to be interpreted in the context of some limitations, as the in vitro assays cannot be compared with clinical and physiological data. On the other hand, in vitro models are the first step to understand the virus–host interactions bringing very useful information to minimize exposure to the virus and the need for assays to be carried out in biosafety laboratories level III. Adding to that, we did not explore the possibility of the antibody dependent enhancement, whereas on the second exposure the major immune response for $CD4^+$ Th1 cells was a good trigger for further investigations.

The use of conditioned medium (CM) obtained from the supernatant derived from cell cultivation has been used to study the effects of those components on in vitro assays to investigate their effects on different cell types [73,74]. However, there is no information about the use of supernatant from PBMC cultivation after SARS-CoV-2 infection/stimulation on alveolar epithelial cells or other cell lines.

In sum, our data brought a new way to explore the effects of SARS-CoV-2 infection on the cellular immune response using a two-step in vitro model, showing the differences between naive response and SARS-CoV-2 primed response. In our Step1 assay, the results showed that natural killer cells played an important role in the immune response for the unexposed individuals and may induce the immune imbalance in COVID-19. $CD4^+$ T lymphocytes producing IFN-γ were the principal phenotype for memory T cells after virus exposure in COVID-19 and can be the key for vaccine development and protective evaluation, as well as the *IFNG* expression with antiviral genes. In our Step2 assay, we observed positive effects on apoptosis reduction in alveolar cells infected by the new coronavirus using the product of virus-specific immune response by people who were exposed previously to SARS-CoV-2, thus suggesting that a second exposure might collaborate with a strong immune response, mainly for those who showed mild symptoms, without hospitalization. Therefore, considering the emergence of new variants, further studies are necessary to the ongoing comprehension of the SARS-CoV-2 immunity even after infection or vaccination. Our findings reinforce that cellular immune response is key to a better understanding of the host interactions in COVID-19. The two-step in vitro models can help

further studies for other immunological assays or might be used as a screening system to test new immunotherapy products.

Author Contributions: J.G.M., T.A., A.M.V.S., A.P.D.A.B. and P.C.C.N. conceived and designed the study. J.G.M., A.M.V.S., T.A., J.H.R.L., T.P.d.S., Y.S.M., S.M.B.d.L., C.B.F. and S.M. performed the cell immunology assays and the first draft writing. M.D.M., A.R.M., B.C.C., J.S.C.C.M. and M.M.S. performed SARS-CoV-2 cultivation, provided the live viral particles to this work, performed the molecular assays to detect SARS-CoV-2, and participated on the first draft writing. T.A., A.M.V.S., C.B.F., T.L.C. and M.O.M. performed molecular immunology assays and interpretation of the data and participated in the first draft writing. J.G.M., T.A., C.B.F., J.d.S., A.F.d.S., L.N.T., T.B.S.P., C.E.L.M., N.F.R. and C.Q.S. performed final cell and molecular assays, and final data interpretation. J.G.M., T.A., A.P.D.A.B., D.B.e.C. and P.C.C.N. wrote and revised the final manuscript. J.G.M. and T.A. have full access to all the data in the study and have final responsibility for the decision to submit for publication. All authors have read and agreed to the published version of the manuscript.

Funding: This research was funded by Instituto de Tecnologia em Imunobiológicos, Bio-Manguinhos, Fundação Oswaldo Cruz, grant number BIO-003-FIO-20 and the APC was funded by Instituto de Tecnologia em Imunobiológicos, Bio-Manguinhos, Fundação Oswaldo Cruz, grant number BIO-003-FIO-20.

Institutional Review Board Statement: The study was conducted according to the guidelines of the Declaration of Helsinki, and approved by the Institutional Review Board of Fundação Oswaldo Cruz (protocol code 34728920.4.0000.5262).

Informed Consent Statement: Informed consent was obtained from all subjects involved in the study.

Data Availability Statement: Not applicable.

Acknowledgments: We thank the Multi-User Research Facility of Biosafety Level III laboratory, Instituto Oswaldo Cruz, Fundação Oswaldo Cruz, Rio de Janeiro, Brazil, especially to Marco A. P. Horta and Keli Antunes for technical assistance. We also would like to thank Leda Castilho, from Universidade Federal do Rio de Janeiro for donation of the spike protein. This work was supported by Instituto Oswaldo Cruz and Instituto de Tecnologia em Imunobiológicos, Bio-Manguinhos, FIOCRUZ (BIO-003-FIO-20). These funding sources had no role in study design, in the collection, analysis and interpretation of data, in the writing of the manuscript and in the decision to submit the article for publication.

Conflicts of Interest: The authors declare that they have no known competing financial interests or personal relationships that could have appeared to influence the work reported in this manuscript.

References

1. Wang, Z.; Yang, B.; Li, Q.; Wen, L.; Zhang, R. Clinical Features of 69 Cases with Coronavirus Disease 2019 in Wuhan, China. *Clin. Infect. Dis.* **2020**, *71*, 769–777. [CrossRef] [PubMed]
2. Prompetchara, E.; Ketloy, C.; Palaga, T. Immune responses in COVID-19 and potential vaccines: Lessons learned from SARS and MERS epidemic. *Asian Pac. J. Allergy Immunol.* **2020**, *38*, 1–9. [CrossRef]
3. Frederiksen, L.S.F.; Zhang, Y.; Foged, C.; Thakur, A. The Long Road toward COVID-19 Herd Immunity: Vaccine Platform Technologies and Mass Immunization Strategies. *Front. Immunol.* **2020**, *11*, 1817. [CrossRef]
4. Fontanet, A.; Cauchemez, S. COVID-19 herd immunity: Where are we? *Nat. Rev. Immunol.* **2020**, *20*, 583–584. [CrossRef]
5. Chung, J.Y.; Thone, M.N.; Kwon, Y.J. COVID-19 vaccines: The status and perspectives in delivery points of view. *Adv. Drug Deliv. Rev.* **2021**, *170*, 1–25. [CrossRef]
6. Giordano, G.; Colaneri, M.; Di Filippo, A.; Blanchini, F.; Bolzern, P.; De Nicolao, G.; Sacchi, P.; Colaneri, P.; Bruno, R. Modeling vaccination rollouts, SARS-CoV-2 variants and the requirement for non-pharmaceutical interventions in Italy. *Nat. Med.* **2021**, *27*, 993–998. [CrossRef]
7. Grech, V.; Souness, J.; Agius, S. Mass population vaccination for COVID-19 in Malta. *J. Vis. Commun. Med.* **2021**, 1–7. [CrossRef]
8. Chibber, P.; Haq, S.A.; Ahmed, I.; Andrabi, N.I.; Singh, G. Advances in the possible treatment of COVID-19: A review. *Eur. J. Pharm.* **2020**, *883*, 173372. [CrossRef]
9. Newton, A.H.; Cardani, A.; Braciale, T.J. The host immune response in respiratory virus infection: Balancing virus clearance and immunopathology. *Semin. Immunopathol.* **2016**, *38*, 471–482. [CrossRef] [PubMed]
10. Coperchini, F.; Chiovato, L.; Croce, L.; Magri, F.; Rotondi, M. The cytokine storm in COVID-19: An overview of the involvement of the chemokine/chemokine-receptor system. *Cytokine Growth Factor Rev.* **2020**, *53*, 25–32. [CrossRef] [PubMed]
11. Julian, B.; Lucie, L.; Marco, F.; Daniel, W.; Philipp, G.; Florian, K.; Stefan, H.; Manuela, D.; Beate, K.; Florent, F.; et al. Presence of SARS-CoV-2-reactive T cells in COVID-19 patients and healthy donors. *medRxiv* **2020**, 20061440. [CrossRef]

12. Chen, Z.; Wherry, E.J. T cell responses in patients with COVID-19. *Nat. Rev. Immunol.* **2020**, *20*, 529–536. [CrossRef] [PubMed]
13. Pontelli, M.C.; Castro, I.A.; Martins, R.B.; Veras, F.P.; La Serra, L.; Nascimento, D.C.; Cardoso, R.S.; Rosales, R.; Lima, T.M.; Souza, J.P.; et al. Infection of human lymphomononuclear cells by SARS-CoV-2. *bioRxiv* **2020**, 225912. [CrossRef]
14. Van Elslande, J.; Vermeersch, P.; Vandervoort, K.; Wawina-Bokalanga, T.; Vanmechelen, B.; Wollants, E.; Laenen, L.; André, E.; Van Ranst, M.; Lagrou, K.; et al. Symptomatic Severe Acute Respiratory Syndrome Coronavirus 2 (SARS-CoV-2) Reinfection by a Phylogenetically Distinct Strain. *Clin. Infect. Dis.* **2021**, *73*, 354–356. [CrossRef]
15. To, K.K.-W.; Hung, I.F.-N.; Ip, J.D.; Chu, A.W.-H.; Chan, W.-M.; Tam, A.R.; Fong, C.H.-Y.; Yuan, S.; Tsoi, H.-W.; Ng, A.C.-K.; et al. Coronavirus Disease 2019 (COVID-19) Re-infection by a Phylogenetically Distinct Severe Acute Respiratory Syndrome Coronavirus 2 Strain Confirmed by Whole Genome Sequencing. *Clin. Infect. Dis.* **2020**, ciaa1275. [CrossRef] [PubMed]
16. Tillett, R.L.; Sevinsky, J.R.; Hartley, P.D.; Kerwin, H.; Crawford, N.; Gorzalski, A.; Laverdure, C.; Verma, S.C.; Rossetto, C.C.; Jackson, D.; et al. Genomic evidence for reinfection with SARS-CoV-2: A case study. *Lancet Infect. Dis.* **2021**, *21*, 52–58. [CrossRef]
17. Ota, M. Will we see protection or reinfection in COVID-19? *Nat. Rev. Immunol.* **2020**, *20*, 351. [CrossRef]
18. Gousseff, M.; Penot, P.; Gallay, L.; Batisse, D.; Benech, N.; Bouiller, K.; Collarino, R.; Conrad, A.; Slama, D.; Joseph, C.; et al. Clinical recurrences of COVID-19 symptoms after recovery: Viral relapse, reinfection or inflammatory rebound? *J. Infect.* **2020**, *81*, 816–846. [CrossRef]
19. Roy, S. COVID-19 Reinfection: Myth or Truth? *SN Compr. Clin. Med.* **2020**, *2*, 710–713. [CrossRef]
20. Jabbari, P.; Rezaei, N. With Risk of Reinfection, Is COVID-19 Here to Stay? *Disaster Med. Public Health Prep.* **2020**, *14*, e33. [CrossRef]
21. Korber, B.; Fischer, W.M.; Gnanakaran, S.; Yoon, H.; Theiler, J.; Abfalterer, W.; Hengartner, N.; Giorgi, E.E.; Bhattacharya, T.; Foley, B.; et al. Tracking Changes in SARS-CoV-2 Spike: Evidence that D614G Increases Infectivity of the COVID-19 Virus. *Cell* **2020**, *182*, 812–827. [CrossRef] [PubMed]
22. Thevarajan, I.; Nguyen, T.H.; Koutsakos, M.; Druce, J.; Caly, L.; van de Sandt, C.E.; Jia, X.; Nicholson, S.; Catton, M.; Cowie, B.; et al. Breadth of concomitant immune responses underpinning viral clearance and patient recovery in a non-severe case of COVID-19. *medRxiv* **2020**. [CrossRef]
23. Wrapp, D.; Wang, N.; Corbett, K.S.; Goldsmith, J.A.; Hsieh, C.-L.; Abiona, O.; Graham, B.S.; McLellan, J.S. Cryo-EM structure of the 2019-nCoV spike in the prefusion conformation. *Science* **2020**, *367*, 1260–1263. [CrossRef] [PubMed]
24. Matos, A.D.R.; Motta, F.C.; Caetano, B.C.; Ogrzewalska, M.; Garcia, C.C.; Lopes, J.C.O.; Miranda, M.; Livorati, M.T.F.P.; Abreu, A.; Brown, D.; et al. Identification of SARS-CoV-2 and additional respiratory pathogens cases under the investigation of COVID-19 initial phase in a Brazilian reference laboratory. *Memórias Inst. Oswaldo Cruz.* **2020**, *115*, 200232. [CrossRef]
25. Paola, C.R.; Edson, D.; Tiago, G.; Daiana, M.; Fernando, d.C.M.; Luciana, R.A.; Anna, C.D.d.P.; Maria, O.; Braulia, C.; Mirleide, C.S.; et al. Genomic surveillance of SARS-CoV-2 reveals community transmission of a major lineage during the early pandemic phase in Brazil. *Evol. Biol.* **2020**. [CrossRef]
26. Son, K.-N.; Liang, Z.; Lipton, H.L. Double-Stranded RNA Is Detected by Immunofluorescence Analysis in RNA and DNA Virus Infections, Including Those by Negative-Stranded RNA Viruses. *J. Virol.* **2015**, *89*, 9383–9392. [CrossRef]
27. Guerreiro, L.T.A.; Robottom-Ferreira, A.B.; Ribeiro-Alves, M.; Toledo-Pinto, T.G.; Brito, T.R.; Rosa, P.S.; Sandoval, F.G.; Jardim, M.R.; Antunes, S.G.; Shannon, E.J.; et al. Gene Expression Profiling Specifies Chemokine, Mitochondrial and Lipid Metabolism Signatures in Leprosy. *PLoS ONE* **2013**, *8*, e64748. [CrossRef]
28. Vandesompele, J.; De Preter, K.; Pattyn, F.; Poppe, B.; Van Roy, N.; De Paepe, A.; Speleman, F. Accurate normalization of real-time quantitative RT-PCR data by geometric averaging of multiple internal control genes. *Genome Biol.* **2002**, *3*, research0034.1. [CrossRef]
29. Pfaffl, M.W. A new mathematical model for relative quantification in real-time RT-PCR. *Nucleic Acids Res.* **2001**, *29*, e45. [CrossRef]
30. Gil Melgaço, J.; E Cunha, D.B.; Azamor, T.; Da Silva, A.M.V.; Tubarão, L.N.; Gonçalves, R.B.; Monteiro, R.Q.; Missailidis, S.; Neves, P.C.D.C.; Bom, A.P.D.A. Cellular and Molecular Immunology Approaches for the Development of Immunotherapies against the New Coronavirus (SARS-CoV-2): Challenges to Near-Future Breakthroughs. *J. Immunol. Res.* **2020**, *2020*, 1–21. [CrossRef]
31. Peng, L.; Liu, J.; Xu, W.; Luo, Q.; Chen, D.; Lei, Z.; Huang, Z.; Li, X.; Deng, K.; Lin, B.; et al. SARS-CoV-2 can be detected in urine, blood, anal swabs, and oropharyngeal swabs specimens. *J. Med. Virol.* **2020**, *92*, 1676–1680. [CrossRef] [PubMed]
32. Wang, Y.; Liu, S.; Liu, H.; Li, W.; Lin, F.; Jiang, L.; Li, X.; Xu, P.; Zhang, L.; Zhao, L.; et al. SARS-CoV-2 infection of the liver directly contributes to hepatic impairment in patients with COVID-19. *J. Hepatol.* **2020**, *73*, 807–816. [CrossRef] [PubMed]
33. Zhang, B.-Z.; Chu, H.; Han, S.; Shuai, H.; Deng, J.; Hu, Y.-F.; Gong, H.-R.; Lee, A.C.-Y.; Zou, Z.; Yau, T.; et al. SARS-CoV-2 infects human neural progenitor cells and brain organoids. *Cell Res.* **2020**, *30*, 928–931. [CrossRef]
34. Giamarellos-Bourboulis, E.J.; Netea, M.G.; Rovina, N.; Akinosoglou, K.; Antoniadou, A.; Antonakos, N.; Damoraki, G.; Gkavogianni, T.; Adami, M.-E.; Katsaounou, P.; et al. Complex Immune Dysregulation in COVID-19 Patients with Severe Respiratory Failure. *Cell Host Microbe* **2020**, *27*, 992–1000.e3. [CrossRef] [PubMed]
35. Zeng, Z.; Xu, L.; Xie, X.; Yan, H.; Xie, B.; Xu, W.; Liu, X.; Kang, G.; Jiang, W.; Yuan, J. Pulmonary pathology of early-phase COVID-19 pneumonia in a patient with a benign lung lesion. *Histopathology* **2020**, *77*, 823–831. [CrossRef] [PubMed]
36. Maucourant, C.; Filipovic, I.; Ponzetta, A.; Aleman, S.; Cornillet, M.; Hertwig, L.; Strunz, B.; Lentini, A.; Reinius, B.; Brownlie, D.; et al. Natural killer cell immunotypes related to COVID-19 disease severity. *Sci. Immunol.* **2020**, *5*, eabd6832. [CrossRef]
37. Gatti, A.; Radrizzani, D.; Viganò, P.; Mazzone, A.; Brando, B. Decrease of Non-Classical and Intermediate Monocyte Subsets in Severe Acute SARS-CoV -2 Infection. *Cytom. Part A* **2020**, *97*, 887–890. [CrossRef]

38. Natalia, F.R.; Carolina, Q.S.; Carlyle, R.L.; Franklin, S.S.; André, C.F.; Mayara, M.; Caroline, S.F.; Vinicius, C.S.; Suelen, S.G.D.; Jairo, R.T.; et al. Atazanavir inhibits SARS-CoV-2 replication and pro-inflammatory cytokine production. *bioRxiv* **2020**, 020925. [CrossRef]
39. Huang, C.; Wang, Y.; Li, X.; Ren, L.; Zhao, J.; Hu, Y.; Zhang, L.; Fan, G.; Xu, J.; Gu, X.; et al. Clinical features of patients infected with 2019 novel coronavirus in Wuhan, China. *Lancet* **2020**, *395*, 497–506. [CrossRef]
40. Merad, M.; Martin, J.C. Pathological inflammation in patients with COVID-19: A key role for monocytes and macrophages. *Nat. Rev. Immunol.* **2020**, *20*, 355–362. [CrossRef]
41. Chen, N.; Zhou, M.; Dong, X.; Qu, J.; Gong, F.; Han, Y.; Qiu, Y.; Wang, J.; Liu, Y.; Wei, Y.; et al. Epidemiological and clinical characteristics of 99 cases of 2019 novel coronavirus pneumonia in Wuhan, China: A descriptive study. *Lancet* **2020**, *395*, 507–513. [CrossRef]
42. Chen, J.; Qi, T.; Liu, L.; Ling, Y.; Qian, Z.; Li, T.; Li, F.; Xu, Q.; Zhang, Y.; Xu, S.; et al. Clinical progression of patients with COVID-19 in Shanghai, China. *J. Infect.* **2020**, *80*, e1–e6. [CrossRef]
43. Yang, X.; Yu, Y.; Xu, J.; Shu, H.; Xia, J.; Liu, H.; Wu, Y.; Zhang, L.; Yu, Z.; Fang, M.; et al. Clinical course and outcomes of critically ill patients with SARS-CoV-2 pneumonia in Wuhan, China: A single-centered, retrospective, observational study. *Lancet Respir. Med.* **2020**, *8*, 475–481. [CrossRef]
44. Zheng, H.-Y.; Zhang, M.; Yang, C.-X.; Zhang, N.; Wang, X.-C.; Yang, X.-P.; Dong, X.-Q.; Zheng, Y.-T. Elevated exhaustion levels and reduced functional diversity of T cells in peripheral blood may predict severe progression in COVID-19 patients. *Cell. Mol. Immunol.* **2020**, *17*, 541–543. [CrossRef]
45. López-Collazo, E.; Avendaño-Ortiz, J.; Martín-Quirós, A.; Aguirre, L.A. Immune Response and COVID-19: A mirror image of Sepsis. *Int. J. Biol. Sci.* **2020**, *16*, 2479–2489. [CrossRef] [PubMed]
46. Liu, L.; Xu, L.; Lin, C. T cell response in patients with COVID-19. *Blood Sci.* **2020**, *2*, 76–78. [CrossRef]
47. Ducloyer, M.; Gaborit, B.; Toquet, C.; Castain, L.; Bal, A.; Arrigoni, P.P.; LeComte, R.; Clement, R.; Sagan, C. Complete post-mortem data in a fatal case of COVID-19: Clinical, radiological and pathological correlations. *Int. J. Leg. Med.* **2020**, *134*, 2209–2214. [CrossRef]
48. Nienhold, R.; Ciani, Y.; Koelzer, V.H.; Tzankov, A.; Haslbauer, J.D.; Menter, T.; Schwab, N.; Henkel, M.; Frank, A.; Zsikla, V.; et al. Two distinct immunopathological profiles in autopsy lungs of COVID-19. *Nat. Commun.* **2020**, *11*, 1–13. [CrossRef]
49. Braun, J.; Loyal, L.; Frentsch, M.; Wendisch, D.; Georg, P.; Kurth, F.; Hippenstiel, S.; Dingeldey, M.; Kruse, B.; Fauchere, F.; et al. SARS-CoV-2-reactive T cells in healthy donors and patients with COVID-19. *Nature* **2020**, *587*, 270–274. [CrossRef] [PubMed]
50. Thieme, C.J.; Anft, M.; Paniskaki, K.; Blazquez-Navarro, A.; Doevelaar, A.; Seibert, F.S.; Hoelzer, B.; Konik, M.J.; Berger, M.M.; Brenner, T.; et al. Robust T Cell Response Toward Spike, Membrane, and Nucleocapsid SARS-CoV-2 Proteins Is Not Associated with Recovery in Critical COVID-19 Patients. *Cell Rep. Med.* **2020**, *1*, 100092. [CrossRef]
51. Zuo, J.; Dowell, A.C.; Pearce, H.; Verma, K.; Long, H.M.; Begum, J.; Aiano, F.; Amin-Chowdhury, Z.; Hoschler, K.; Brooks, T.; et al. Robust SARS-CoV-2-specific T-cell immunity is maintained at 6 months following primary infection. *Nat. Immunol.* **2020**, *22*, 620–626. [CrossRef]
52. Mateus, J.; Grifoni, A.; Tarke, A.; Sidney, J.; Ramirez, S.I.; Dan, J.M.; Burger, Z.C.; Rawlings, S.A.; Smith, D.M.; Phillips, E.; et al. Selective and cross-reactive SARS-CoV-2 T cell epitopes in unexposed humans. *Science* **2020**, *370*, 89–94. [CrossRef] [PubMed]
53. Grifoni, A.; Weiskopf, D.; Ramirez, S.I.; Mateus, J.; Dan, J.M.; Moderbacher, C.R.; Rawlings, S.A.; Sutherland, A.; Premkumar, L.; Jadi, R.S.; et al. Targets of T Cell Responses to SARS-CoV-2 Coronavirus in Humans with COVID-19 Disease and Unexposed Individuals. *Cell* **2020**, *181*, 1489–1501.e15. [CrossRef] [PubMed]
54. Tay, M.Z.; Poh, C.M.; Rénia, L.; Macary, P.A.; Ng, L.F.P. The trinity of COVID-19: Immunity, inflammation and intervention. *Nat. Rev. Immunol.* **2020**, *20*, 363–374. [CrossRef]
55. Gil Melgaço, J.; Azamor, T.; Bom, A.P.D.A. Protective immunity after COVID-19 has been questioned: What can we do without SARS-CoV-2-IgG detection? *Cell. Immunol.* **2020**, *353*, 104114. [CrossRef] [PubMed]
56. Kaneko, N.; Kuo, H.-H.; Boucau, J.; Farmer, J.R.; Allard-Chamard, H.; Mahajan, V.S.; Piechocka-Trocha, A.; Lefteri, K.; Osborn, M.; Bals, J.; et al. Loss of Bcl-6-Expressing T Follicular Helper Cells and Germinal Centers in COVID-19. *Cell* **2020**, *183*, 143–157.e13. [CrossRef]
57. Meckiff, B.J.; Ramírez-Suástegui, C.; Fajardo, V.; Chee, S.J.; Kusnadi, A.; Simon, H.; Grifoni, A.; Pelosi, E.; Weiskopf, D.; Sette, A.; et al. Single-Cell Transcriptomic Analysis of SARS-CoV-2 Reactive CD4 + T Cells. *Soc. Sci. Res. Netw.* **2020**, *7*, 3641939. [CrossRef]
58. Zhou, Y.; Fu, B.; Zheng, X.; Wang, D.; Zhao, C.; Qi, Y.; Sun, R.; Tian, Z.; Xu, X.; Wei, H. Pathogenic T-cells and inflammatory monocytes incite inflammatory storms in severe COVID-19 patients. *Natl. Sci. Rev.* **2020**, *7*, 998–1002. [CrossRef]
59. Pia, L. SARS-CoV-2-reactive T cells in patients and healthy donors. *Nat. Rev. Immunol.* **2020**, *20*, 353. [CrossRef]
60. Oestreich, K.J.; Weinmann, A.S. Transcriptional mechanisms that regulate T helper 1 cell differentiation. *Curr. Opin. Immunol.* **2012**, *24*, 191–195. [CrossRef]
61. De Araújo-Souza, P.S.; Hanschke, S.C.H.; Viola, J. Epigenetic Control of Interferon-Gamma Expression in CD8 T Cells. *J. Immunol. Res.* **2015**, *2015*, 849573. [CrossRef]
62. Pulko, V.; Davies, J.S.; Martinez, C.; Lanteri, M.C.; Busch, M.C.L.M.P.; Diamond, M.S.; Knox, K.; Bush, E.C.; Sims, P.; Sinari, S.; et al. Human memory T cells with a naive phenotype accumulate with aging and respond to persistent viruses. *Nat. Immunol.* **2016**, *17*, 966–975. [CrossRef] [PubMed]

63. Mueller, S.N.; Gebhardt, T.; Carbone, F.R.; Heath, W. Memory T Cell Subsets, Migration Patterns, and Tissue Residence. *Annu. Rev. Immunol.* **2013**, *31*, 137–161. [CrossRef] [PubMed]
64. Raeber, M.E.; Zurbuchen, Y.; Impellizzieri, D.; Boyman, O. The role of cytokines in T-cell memory in health and disease. *Immunol. Rev.* **2018**, *283*, 176–193. [CrossRef]
65. Stephens, D.S.; McElrath, M.J. COVID-19 and the Path to Immunity. *JAMA* **2020**, *324*, 1279. [CrossRef] [PubMed]
66. Lee, M.; Wang, C.; Jin, S.W.; Labrecque, M.; Beischlag, T.V.; Brockman, M.A.; Choy, J.C. Expression of human inducible nitric oxide synthase in response to cytokines is regulated by hypoxia-inducible factor-1. *Free Radic. Biol. Med.* **2019**, *130*, 278–287. [CrossRef]
67. Kaplan, A.; Ciftci, G.A.; Kutlu, M. The apoptotic and genomic studies on A549 cell line induced by silver nitrate. *Tumor Biol.* **2017**, *39*, 101042831769503. [CrossRef]
68. Chu, S.C.; Marks-Konczalik, J.; Wu, H.-P.; Banks, T.C.; Moss, J. Analysis of the Cytokine-Stimulated Human Inducible Nitric Oxide Synthase (iNOS) Gene: Characterization of Differences between Human and Mouse iNOS Promoters. *Biochem. Biophys. Res. Commun.* **1998**, *248*, 871–878. [CrossRef]
69. Zeng, M.; Huang, C.; Zheng, H.; Chen, Q.; He, W.; Deng, Y. Effects of Ghrelin on iNOS-Derived NO Promoted LPS-Induced Pulmonary Alveolar Epithelial A549 Cells Apoptosis. *Cell. Physiol. Biochem.* **2018**, *49*, 1840–1855. [CrossRef]
70. Korhonen, R.; Linker, K.; Pautz, A.; Förstermann, U.; Moilanen, E.; Kleinert, H. Post-Transcriptional Regulation of Human Inducible Nitric-Oxide Synthase Expression by the Jun N-terminal Kinase. *Mol. Pharm.* **2007**, *71*, 1427–1434. [CrossRef]
71. Stefano, G.B.; Esch, T.; Kream, R.M. Potential Immunoregulatory and Antiviral/SARS-CoV-2 Activities of Nitric Oxide. *Med. Sci. Monit.* **2020**, *26*, e925679-1–e925679-3. [CrossRef] [PubMed]
72. Akaberi, D.; Krambrich, J.; Ling, J.; Luni, C.; Hedenstierna, G.; Järhult, J.D.; Lennerstrand, J.; Lundkvist, Å. Mitigation of the replication of SARS-CoV-2 by nitric oxide in vitro. *Redox Biol.* **2020**, *37*, 101734. [CrossRef] [PubMed]
73. Lange-Consiglio, A.; Gusmara, C.; Manfredi, E.; Idda, A.; Soggiu, A.; Greco, V.; Bonizzi, L.; Cremonesi, F.; Zecconi, A. Antimicrobial Effects of Conditioned Medium From Amniotic Progenitor Cells in vitro and in vivo: Toward Tissue Regenerative Therapies for Bovine Mastitis. *Front. Vet. Sci.* **2019**, *6*, 443. [CrossRef] [PubMed]
74. Crunfli, F.; Carregari, V.C.; Veras, F.P.; Vendramini, P.H.; Valença, A.G.; Antunes, A.S.; Brandão-Teles, C.; da Silva Zuccoli, G.; Reis-de-Oliveira, G.; Silva-Costa, L.C.; et al. SARS-CoV-2 infects brain astrocytes of COVID-19 patients and impairs neuronal viability. *medRxiv* **2020**. [CrossRef]